THE UNIVERSITY OF MICHIGAN

COLLEGE OF ENGINEERING

DEPARTMENT OF ELECTRICAL ENGINEERING

Radiation Laboratory

VOR PARASITIC LOOP COUNTERPOISE SYSTEMS - II

Interim Report No. 3

(1 February - 30 April 1970)

By

Dipak L. Sengupta and Joseph E. Ferris

15 May 1970

Contract FA 69-WA-2085, Project 330-001-03N

Contract Monitor: Mr. Sterling Anderson

Contract With: Federal Aviation Administration
Radar and Navaids Section
800 Independence, SW
Washington, DC 20590

Administered through:

OFFICE OF RESEARCH ADMINISTRATION • ANN ARBOR

1. Introduction

This is the Third Interim Report on Contract FA 69-WA-2085, Project 330-001-03N "VOR Parasitic Loop Counterpoise Systems-II," and covers the period 1 February to 30 April 1970.

During this period we have developed theoretical expressions for the radiation field produced by a loop counterpoise antenn having a figure-of-eight type of radiation pattern in the azimuthal plane. This is the type of antenna which is in actual use in an existing VOR system. The theoretical patterns have been compared with measured results at the frequency 1080 MHz. Excellent agreement has been obtained between the two. As far as we are aware, this is the first time that an accurate theory has been given for the existing VOR antenna radiation patterns. This theory has been modified and generalized to the case of the parasitic loop counterpoise antenna with a figure-of-eight type of excitation. Theoretical patterns obtained from numerical computation of these expressions are given for some typical cases.

The experimental investigation during this period has been directed towards the 15' diameter counterpoise case. This has been done to develop the appropriate parameters for the full scale parasitic loop counterpoise antenna.

2. VOR Antenna Radiation Patterns

In this section we develop and discuss the theoretical expressions for the radiation field produced by existing VOR antennas. Such an antenna consists of a pair of Alford loops suitably excited and placed at a convenient height above a circular ground plane or counterpoise. We refer to this antenna as the loop counterpoise antenna. The two Alford loops lie in the same plane which is parallel to the plane of the counterpoise. The Alford

loops are separated by a distance , 2d , small compared to a wavelength and are excited with signals having equal amplitude but opposite phase. Thus the free space azimuthal pattern of the antenna would be a figure-of-eight.

2.1 Theory

For the purpose of theoretical analysis the VOR loop counterpoise antenna is replaced by a point source with appropriate far field variation placed above the counterpoise as shown in Fig. 1.

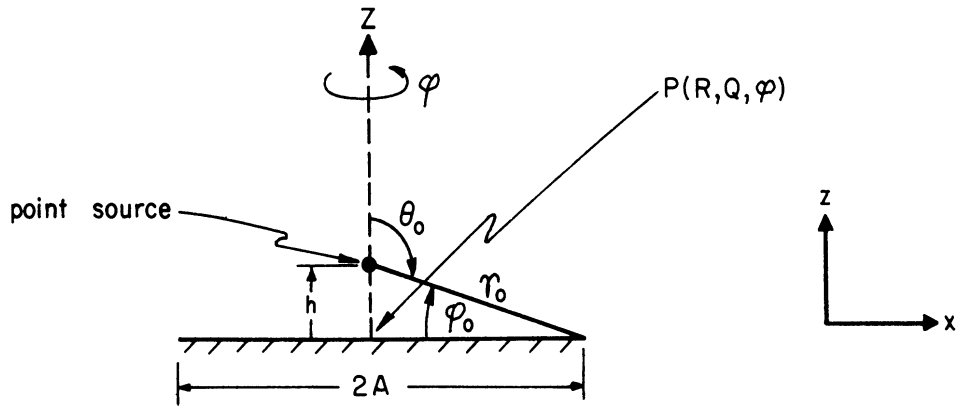

Figure 1

The free space radiation field of the point source (in the absence of the counterpoise) can be represented by:

$$E^i_\phi = \eta_o I_o \left(\frac{ka}{2}\right)^2 f(\theta,\phi)\sin\theta \frac{e^{ikR}}{R} \quad , \tag{2.1}$$

where,

R, θ, ϕ are the usual spherical coordinates of the far field point with origin at the point source,

η_o is the intrinsic impedance of free space,

$k = 2\pi/\lambda$ is the free space propagation constant,

I_o is the amplitude of the current in the Alford loops,

a is the equivalent radius of the Alford loop,

$f(\theta,\phi)$ is the pattern function which is determined by the method of excitation and orientation of the two loops.

Note that the field in (2.1) is polarized in the ϕ-direction. The symmetry of the system dictates that the far field produced by the antenna shown in Fig. 1 will also be polarized in the ϕ-direction. In the present case, the two Alford loops are excited with equal amplitudes but opposite phase so that $f(\theta,\phi)$ can be written explicitly as follows:

$$f(\theta,\phi) = 2\, i \sin (kd \sin\theta \cos\phi) \quad . \tag{2.2}$$

Equation (2.2) means that in the azimuthal plane $\theta = \pi/2$, the pattern is a figure-of-eight having a maximum along the x-axis.

With the incident field given by (2.1), the far field produced by the loop counterpoise antenna shown in Fig. 1 can be obtained by applying the concepts of geometrical theory of diffraction and the

results of Sommerfeld's theory for half-plane diffraction. We do not give the details of the method here since it has been discussed in a previous report (Sengupta et al, 1968) where it was assumed that $f(\theta,\phi) \equiv 1$.

It can be shown that the far field expression valid in the transition region and defined by $\frac{\pi}{2} - \phi_o \leq \theta \leq \frac{\pi}{2} + \phi_o$, is given by

$$E_\phi \sim \eta_o I_o \left(\frac{ka}{2}\right)^2 f(\theta_o,\phi) \frac{e^{ik(R-A\sin\theta)}}{R\sqrt{\sin\theta}} \left[U(r_o,\psi_1)-U(r_o,\psi_2)\right] , \quad (2.3)$$

where

$$U(r,\psi)=e^{-ikr\cos\psi} \left(\frac{1-i}{2}\right) \int_{-\infty}^{p} e^{i\pi\frac{t^2}{2}} dt , \quad (2.4)$$

$$\psi_1 = \phi_o - \frac{\pi}{2} - \theta, \qquad \psi_2 = \phi_o + \frac{\pi}{2} + \theta \quad (2.5)$$

$$p = 2\left(\frac{kR}{\pi}\right)^{1/2} \cos\frac{\psi}{2} . \quad (2.6)$$

The near edge diffracted field valid in the region $0 \leq \theta \leq \frac{\pi}{2} - \phi_o$ is given by:

$$E_{\phi_N} \sim \eta_o I_o \left(\frac{ka}{2}\right)^2 f(\theta_o,\phi) \cdot \frac{\cos\theta \sin\left(\frac{\phi_o}{2}\right)}{\cos\phi_o - \sin\theta}$$

$$\times \left[\frac{\cos^3\phi_o}{\pi k r_o \sin\theta(1-\sin\theta)}\right]^{1/2} \frac{e^{i\frac{\pi}{4}} e^{ik(R-A\sin\theta+r_o)}}{R} . \quad (2.7)$$

The far edge diffracted field valid in the region $0 \leq \theta \leq \frac{\pi}{2} - \phi_o$ is given by:

$$E_{\phi_F} \sim -\eta_o I_o \left(\frac{ka}{2}\right)^2 \cdot f(\theta_o, \phi) \cdot \frac{e^{-i\left(\frac{\pi}{4} - kA\sin\theta\right)} e^{ikr_o}}{\sqrt{\pi kr_o \sin\theta}} \frac{e^{ikR}}{R}$$

$$\times \frac{\cos^{3/2}\phi_o}{\cos\phi_o + \sin\theta} \frac{\cos\theta \sin\left(\frac{\phi_o}{2}\right)}{\sqrt{1+\sin\theta}} \quad . \qquad (2.8)$$

With the above field expressions it is now possible to develop a single expression for the far field which is valid in the region $0 < \theta < \pi$. This can be done by starting from the transition region field given by (2.3) and modifying it to account for the different contributions in the various regions of space. The complete far field expression, thus obtained, can be expressed as:

$$E_\phi \sim \eta_o I_o \left(\frac{ka}{2}\right)^2 \cdot \frac{e^{i(kR-\pi/4)}}{R} S^A(\theta) \quad , \qquad (2.9)$$

where,

$$S^A(\theta) = \left\{ \frac{F^o(\theta) \sin\theta f(\theta,\phi) e^{-ikA\sin\theta}}{\sqrt{2}} + \frac{|\cos\theta| \sin\left(\frac{\phi_o}{2}\right)}{\sqrt{\pi kr_o \sin\theta}} e^{ikr_o} L^o(\theta) \right\} \quad , \qquad (2.10)$$

$$F^o(\theta) = e^{ikr_o \sin(\theta - \phi_o)} \int_{-\infty}^{p_1} e^{i\frac{\pi t^2}{2}} dt$$

$$- e^{ikr_o \sin(\theta + \phi_o)} \cdot \int_{-\infty}^{p_2} e^{i\frac{\pi t^2}{2}} dt \quad , \qquad (2.11)$$

$$L^{o}(\theta) = \frac{e^{i(\frac{\pi}{2} - kA\sin\theta)}}{\sqrt{1-\sin\theta}} \frac{f(\theta_o, \phi)\cos^{3/2}\phi_o - f(\theta,\phi)\sin^{3/2}\theta}{\cos\phi_o - \sin\theta}$$

$$- \frac{e^{ikA\sin\theta}}{\sqrt{1+\sin\theta}} \frac{f(\theta_o,\phi)\cos^{3/2}\phi_o}{\cos\phi_o + \sin\theta} , \qquad (2.12)$$

$$f(\theta,\phi = 2i \sin(kd\sin\theta\cos\phi) . \qquad (2.13)$$

Equations (2.9) through (2.13) have been used to compute the far field field pattern produced by loop counterpoise antennas that are used in existing VOR antennas. To the best of our knowledge the expressions given above are new and appear here for the first time.

2.2 Comparison Between Theory and Experiment

The measured free space far field elevation patterns of loop counterpoise antennas are shown in Figs. 2, 3 and 4 for three selected values of the counterpoise diameter. All the patterns have been measured in the x-z plane of Fig. 1 and at the frequency of 1080 MHz. The corresponding theoretical patterns as obtained by numerical computation of Eqs. (2.9) through (2.13) are also shown in Figures 2 through 4 for comparison. The agreement between theory and experiment for the cases with kA = 17.92 (2A = 5.2') and kA = 51.69 (2A = 15') may be considered to be very good. The minor lobes in the pattern in directions $\theta > \pi/2$, as well as the kink in the pattern near $\theta \simeq \pi/2$ for the case kA = 51.69 are attributed to the outside pattern range and the feed system. The agreement between theory and experiment for the case kA = 6.32 (2A = 22") is not as good although it may be considered to be fair over

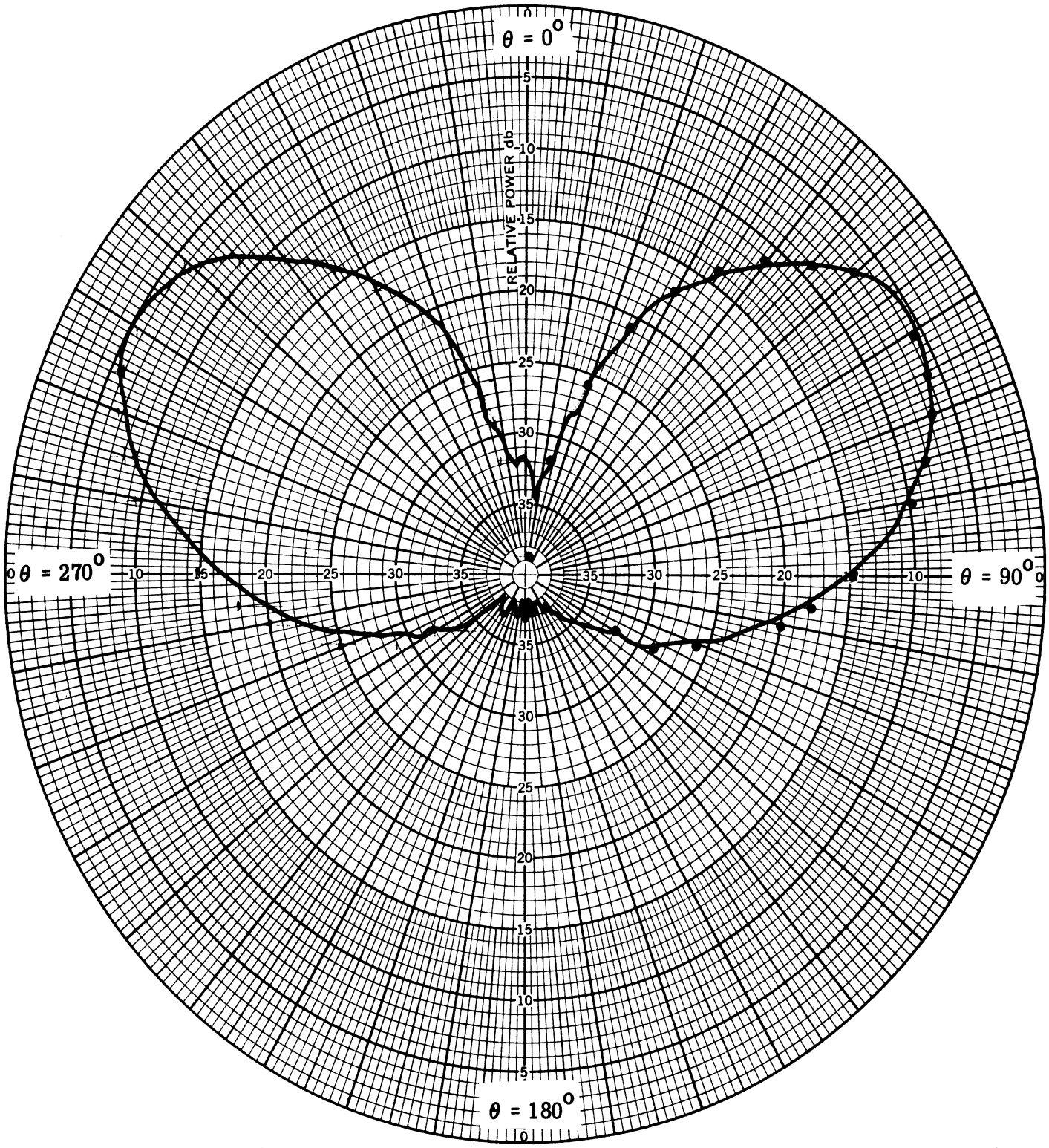

FIG. 2: Far-Field Elevation Pattern of a Non-uniformly Excited Loop Counterpoise Antenna. kh = 2.75, kd = 0.92, f = 1080 MHz, ka = 17.92 ——— Experimental, • • • • Theoretical.

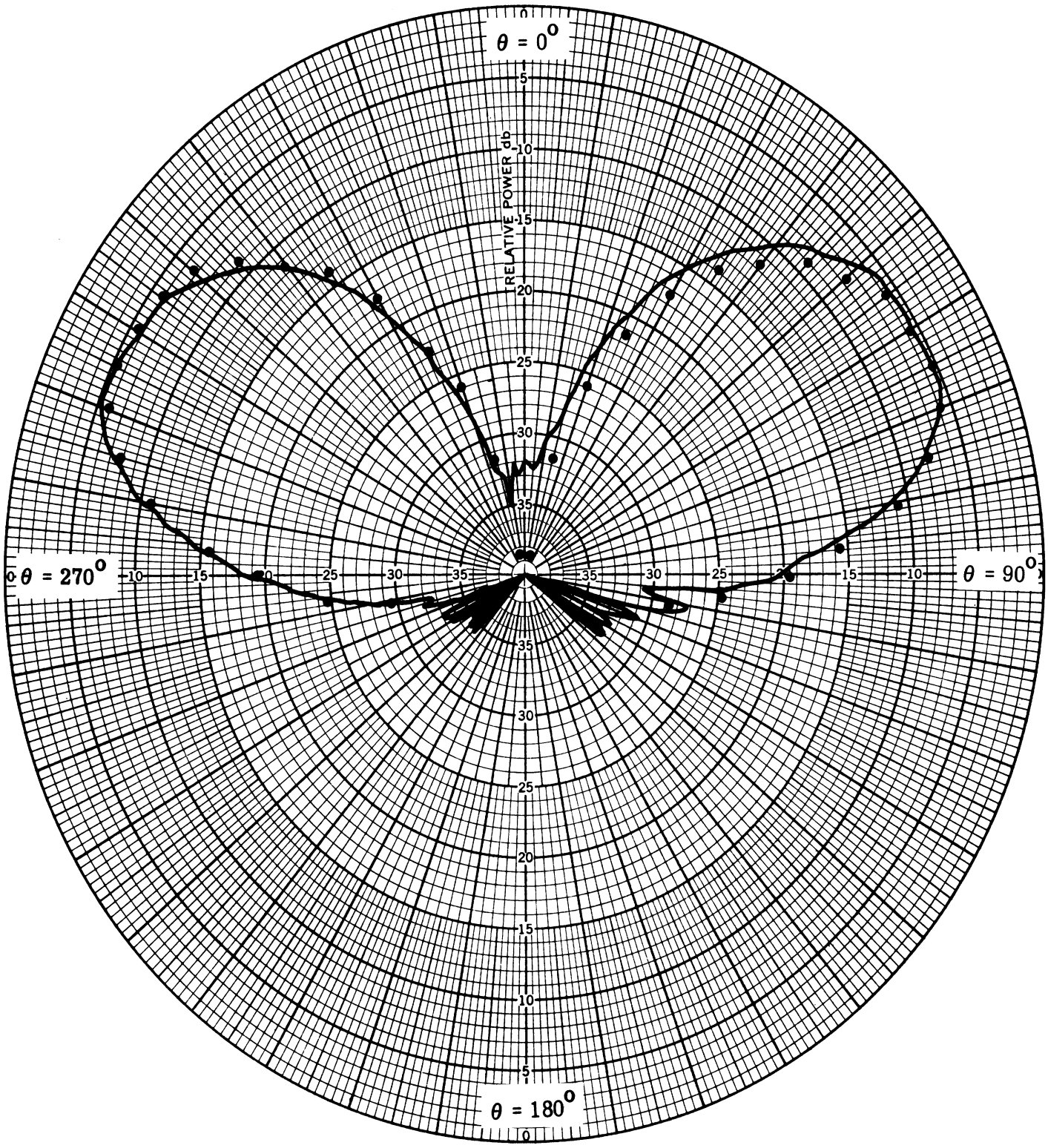

FIG. 3: Far-Field Elevation Pattern of a Non-uniformly Excited Loop Counterpoise Antenna. kh = 2.75, kd = 0.92, f = 1080 MHz kA = 51.69 ——— Experimental • • • • Theoretical.

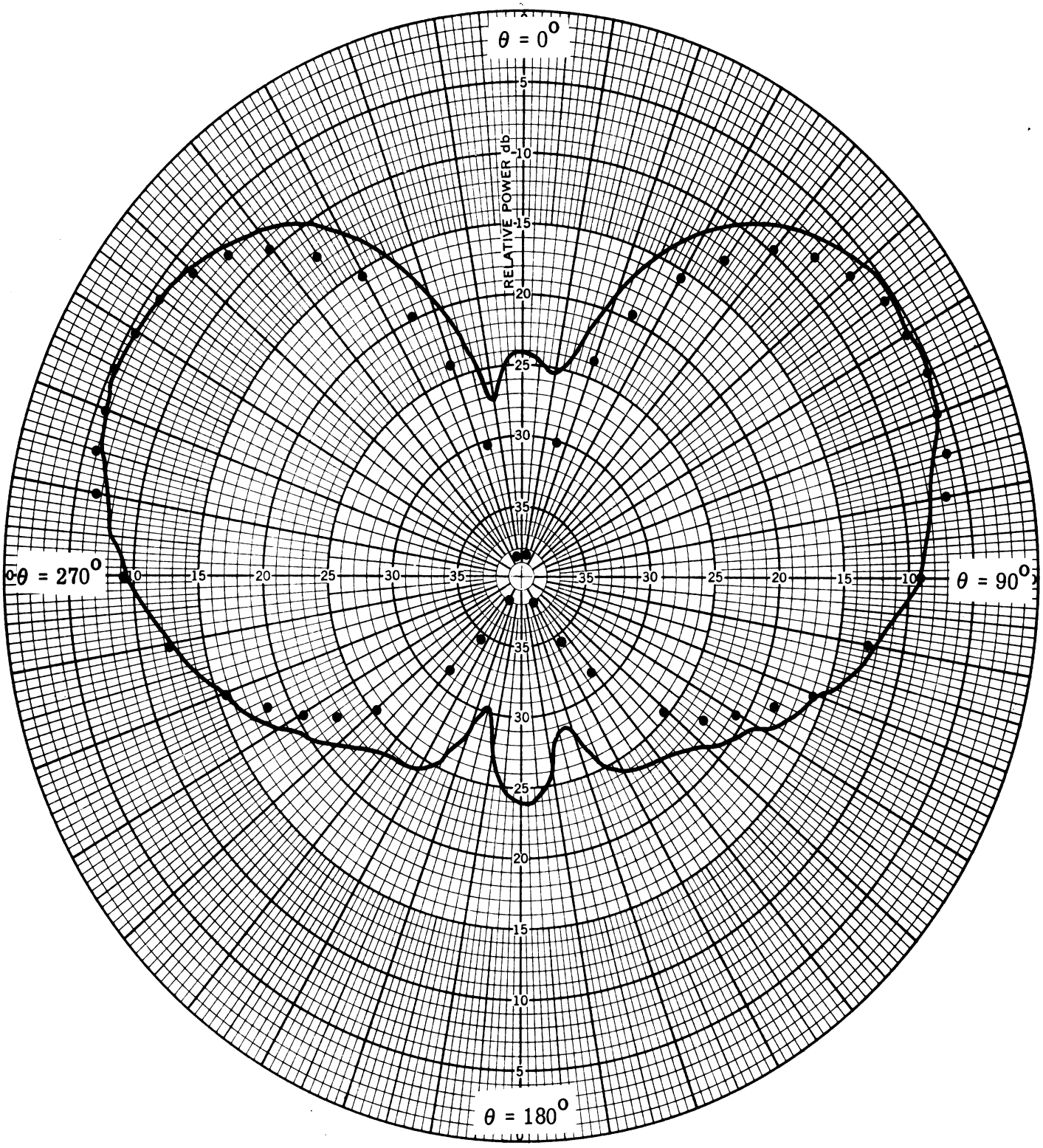

FIG. 4: Far-Field Elevation Pattern of a Non-uniformly Excited Loop Counterpoise Antenna. kh = 2.75, kd = 0.92, f = 1080 MHz, ka = 6.32, —— Experimental • • • • Theoretical .

most of the region. The reason for this is due to the small size of the counterpoise for which the theory becomes poor. It may be concluded from the results given in this section that the present theory can be used with sufficient accuracy to compute existing VOR antenna patterns having counterpoise $2A \geq 22''$; the theory becomes more accurate for large counterpoises.

3. Non-Uniformly Excited Parasitic Loop Counterpoise Antenna Patterns

In this section we give the theoretical expressions for the radiation field produced by non-uniformly excited parasitic loop counterpoise antennas. The theoretical model of a single parasitic loop counterpoise antenna is shown in Fig. 5. A double parasitic loop counterpoise antenna may be obtained from Fig. 5 by inserting another parasitic loop at the appropriate place.

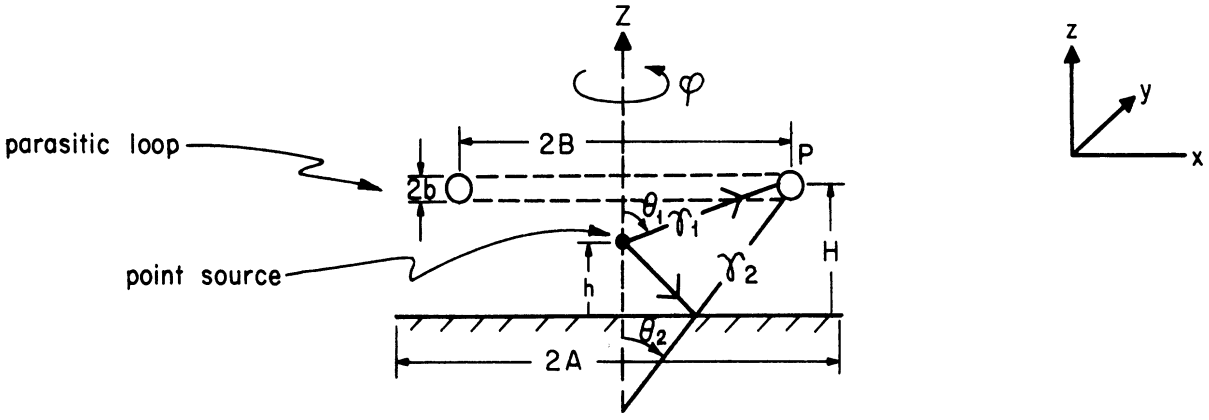

Figure 5

3.1 Single Parasitic Loop Counterpoise Antenna Pattern

As before, the free space far field produced by the excited elements only (represented by the point source in Fig. 5) is:

$$E_{\phi}^{i} = \eta_o I_o \left(\frac{ka}{2}\right)^2 \cdot f(\theta,\phi) \sin\theta \frac{e^{ikR}}{R} \quad , \tag{3.1}$$

where

$$f(\theta,0) = 2i \sin(kd \sin\theta \cos\phi) \quad . \tag{3.2}$$

The first step in the analysis involves the determination of the current induced in the parasitic element.

Parasitic Current. Let the total field incident at the point P on the parasitic loop be denoted by $E_{\phi}^{inc}(P)$. Then the parasitic current I_{P_o} is given by

$$I_{P_o} = \frac{2\pi}{i\eta_o kM} E_{\phi}^{inc}(P) \tag{3.3}$$

where

$$M = 0.577 + \ln\left(\frac{kb}{2}\right) - i\frac{\pi}{2} \quad . \tag{3.4}$$

The basis and nature of approximations involved in (3.3) has been discussed elsewhere (Sengupta and Weston, 1969) and will not be reported here.

The incident field $E_{\phi}^{inc}(P)$ consists of direct, reflected and diffracted fields. The derivation of the different field components that would be used in obtaining the parasitic current are shown in Fig. 6. Thus $E_{\phi}^{inc}(P)$ can be written formally as follows:

$$E_{\phi}^{inc}(P) = E_{\phi}^{12}(P) + E_{\phi}^{56}(P) \quad . \tag{3.5}$$

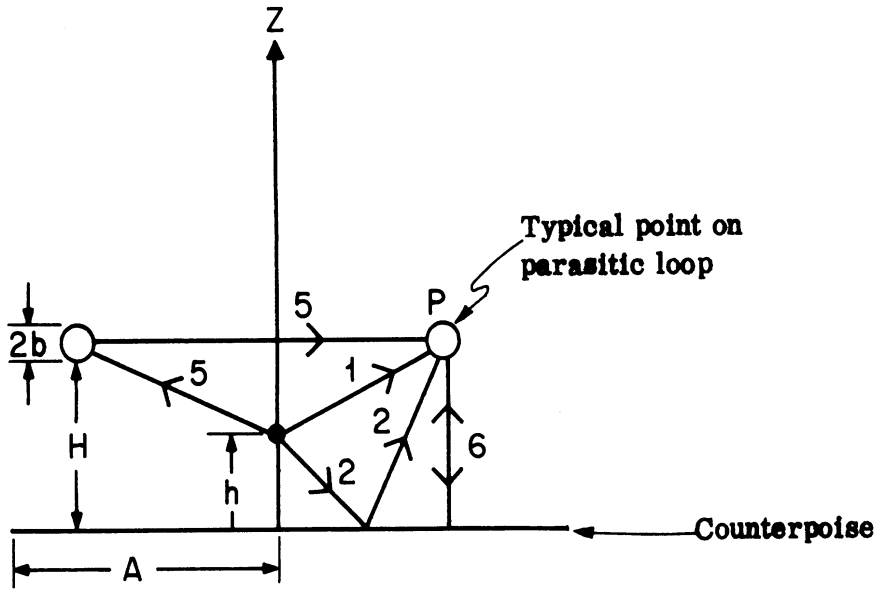

Figure 6

Explicit expressions for the component fields $E_\phi^{12}(P)$ and $E_\phi^{56}(P)$ can be obtained by following the method discussed by Sengupta et al (1968) and by Sengupta and Weston (1969). These expressions are;

$$E_\phi^{12}(P) = \eta_o I_o \left(\frac{ka}{2}\right)^2 \left[f(\theta_1, \phi) \frac{B}{r_1} \frac{e^{ikr_1}}{r_1} - f(\theta_2, \phi) \frac{B}{r_2} \frac{e^{ikr_2}}{r_2} \right], \quad (3.6)$$

where

$$r_1^2 = B^2 + (H-h)^2 \quad , \quad r_2^2 = B^2 + (H+h)^2 \quad , \quad (3.7)$$

$$E_{\phi}^{56}(P) = -\eta_o I_o \left(\frac{ka}{2}\right)^2 \frac{\pi}{2iM} f(\theta_1, \phi) \cdot \frac{B}{r_1} \frac{e^{ikr_1}}{r_1}$$

$$\times \left[\left(\frac{1}{\pi kB}\right)^{1/2} e^{i(2kB+\frac{\pi}{4})} - \left(\frac{1}{\pi kH}\right)^{1/2} e^{i(2kH-\frac{\pi}{4})} \right] . \qquad (3.8)$$

Using (3.3) and (3.6) through (3.8) it can be shown that

$$I_{P_o} = I_{P_o}^{12} + I_{P_o}^{56} , \qquad (3.9)$$

where

$$I_{P_o}^{12} = I_o \left(\frac{ka}{2}\right)^2 \frac{2\pi B}{ikM} \left[f(\theta_1, \phi) \frac{e^{ikr_1}}{r_1} - f(\theta_2, \phi) \frac{e^{ikr_2}}{r_2} \right] , \qquad (3.10)$$

$$I_{P_o}^{56} = I_o \left(\frac{ka}{2}\right)^2 \cdot \frac{\pi^2 (kB)}{M^2} \frac{e^{ikr_1}}{(kr_1)^2} f(\theta_1, \phi)$$

$$\times \left[\left(\frac{1}{\pi kB}\right)^{1/2} e^{i(2kB+\frac{\pi}{4})} - \left(\frac{1}{\pi kH}\right)^{1/2} e^{i(2kH-\frac{\pi}{4})} \right] . \qquad (3.11)$$

We now make the following approximation valid for $kd \ll 1$,

$$f(\theta_1, \phi) = 2i \sin (kd \sin\theta_1 \cos \phi)$$

$$\simeq f(\theta_1) \cos \phi , \qquad (3.12)$$

$$f(\theta_2, \phi) \simeq f(\theta_2) \cos \phi , \qquad (3.13)$$

where

$$f(\theta_1) = 2i\, kd \sin\theta_1 = 2i\, (kd) \frac{B}{r_1} , \qquad (3.14)$$

$$f(\theta_2) = 2i\, kd \sin\theta_2 = 2i\, (kd) \frac{B}{r_2} . \qquad (3.15)$$

After introducing (3.12) through (3.15) into (3.10 and (3.11) we obtain

$$I_{P_o}^{12} = I_o \left(\frac{ka}{2}\right)^2 \frac{2\pi B}{2} \left[f(\theta_1) \frac{e^{ikr_1}}{r_1^2} - f(\theta_2) \frac{e^{ikr_2}}{r_2^2} \right] \cos\phi \qquad (3.16)$$

$$I_{P_o}^{56} = I_o \left(\frac{ka}{2}\right)^2 \frac{\pi^2 (kB)}{M^2} \frac{e^{ikr_1}}{(kr_1)^2} \cdot f(\theta_1)$$

$$\times \left[\left(\frac{1}{\pi kB}\right)^{1/2} e^{i(2kB+\frac{\pi}{4})} - \left(\frac{1}{\pi kH}\right)^{1/2} e^{i(2kH-\frac{\pi}{4})} \right] \cos\phi \, . \qquad (3.17)$$

Thus we can write the parasitic current expression I_{P_o} in the following form.

$$I_{P_o} = I_{P_o}^{12} + I_{P_o}^{56} = I_{P_o}^{\pi} \cos\phi \, , \qquad (3.18)$$

where explicit expression for $I_{P_o}^{\pi}$ may be obtained after introducing Eqs. (3.16) and (3.17) into (3.18). It is important to note here that due to the nature of excitation, the parasitic current is not independent of ϕ. This completes the derivation of the theoretical expressions for the current induced in the parasitic loop in a single parasitic loop counterpoise antenna with figure-of-eight type excitation.

The Radiation Field. The complete radiation field produced by a non-uniformly excited single parasitic loop counterpoise antenna is obtained by vectorially adding the individual fields produced by the pair of Alford loops above the counterpoise and the parasitic loop above the counterpoise. The Alford loop counterpoise field is as given in the previous section. The parasitic field expression is derived below.

The free space radiation field produced by a circular loop carrying a current of the form given by Eq. (3.18) has been discussed earlier (Sengupta , 1969). In general the far electric fields are:

$$E_{\phi}^{i} \sim i\eta_0 I'_{P_0} \left(\frac{kB}{2}\right) J_1' (kB \sin\theta)\cos\phi \, \frac{e^{ikR}}{R} \quad , \tag{3.19}$$

$$E_{\theta}^{i} \sim i\eta_0 I'_{P_0} \left(\frac{kB}{2}\right) \frac{J_1(kB\sin\theta)}{(kB\sin\theta)} \cos\theta \sin\phi \frac{e^{ikR}}{R} \quad , \tag{3.20}$$

where

R, θ, ϕ are the usual spherical coordinates of the far field point with origin in the center of the parasitic loop which lines in the x-y plane, and

J_1 is the first order Bessel function of the first kind.

For obtaining the principal plane field we are interested in the $\phi = 0^o$ plane and thus we have:

$$E_{\phi}^{i} \sim i\eta_0 I'_{P_0} \left(\frac{kB}{2}\right) \frac{e^{ikR}}{R} J_1' (kB\sin\theta) \tag{3.21}$$

$$E_{\theta}^{i} \equiv 0 \, .$$

Let us obtain the ϕ-component of the field. With the incident field given by (3.19) it can be shown that the far field produced by the parasitic loop above the counterpoise is given by the following expression valid in the region $0 < \theta < \pi$,

$$E_{\phi}^{P} \sim \eta_0 I'_{P_0} \left(\frac{kB}{2}\right) \frac{e^{i(kR-\frac{\pi}{4})}}{R} \; i\, F(\theta) \cos\phi \quad , \tag{3.22}$$

where

$$F(\theta) = \frac{J_1'(kB\sin\theta)}{\sqrt{2}}\, F^P(\theta) e^{-ikA\sin\theta} + \frac{|\cos\theta|\sin(\frac{\phi_P}{2})}{\sqrt{\pi kr_P \sin\theta}}\, e^{ikr_P} L^P(\theta)\,, \tag{3.23}$$

$$L^P(\theta) = \frac{e^{i(\frac{\pi}{2} - kA\sin\theta)}}{\sqrt{1-\sin\theta}} \left[\frac{\cos^{1/2}\phi_P J_1'(kB\cos\phi_P) - \sin^{1/2}\theta\, J_1'(kB\sin\theta)}{\cos\phi_P - \sin\theta} \right]$$

$$- \frac{e^{-ikA\sin\theta}}{\sqrt{1+\sin\theta}}\,, \tag{3.24}$$

$$F^P(\theta) = e^{ikr_p\sin(\theta-\phi_P)} \int_{-\infty}^{p_5} e^{i\frac{\pi t^2}{2}} dt - e^{ikr_P\sin(\theta+\phi_P)} \int_{-\infty}^{p_6} e^{i\frac{\pi t^2}{2}} dt \tag{3.25}$$

$$p_5 = 2(\frac{kr_P}{\pi})^{1/2} \cos(\frac{\phi_P - \theta - \frac{\pi}{2}}{2})\,, \quad p_6 = 2(\frac{kr_P}{\pi})^{1/2} \cos(\frac{\phi_P + \theta + \frac{\pi}{2}}{2})\,, \tag{3.26}$$

$$r_P^2 = A^2 + H^2\,, \quad \tan\phi_P = \frac{H}{A}\,. \tag{3.27}$$

The complete far field is now obtained by combining Eqs. (2.9) and (3.22). It can be written formally as:

$$E_\phi \sim \eta_o I_o (\frac{ka}{2})^2 \frac{e^{i(kR - \frac{\pi}{4})}}{R}\, S(\theta)\,, \tag{3.28}$$

where

$$S(\theta) = S^A(\theta) + S_{12}^P(\theta) + S_{56}^P(\theta)\,. \tag{3.29}$$

Explicit expressions for $S^A(\theta)$ are given by Eqs. (2.10) through (2.13). The last two terms on the right-hand side of (3.29) are given by:

$$S_{12}^P(\theta) = \frac{\pi(kB)^2}{M}\left[f(\theta_1)\frac{e^{ikr_1}}{(kr_1)^2} - f(\theta_2)\frac{e^{ikr_2}}{(kr_2)^2}\right]F(\theta)\cos\phi \qquad (3.30)$$

$$S_{56}^P(\theta) = \frac{i\pi^2(kB)^2}{2M^2}\frac{e^{ikr_1}}{(kr_1)^2}f(\theta_1)$$

$$\times\left[\left(\frac{1}{\pi kB}\right)^{1/2} e^{i(2kB+\frac{\pi}{4})} - \left(\frac{1}{\pi kH}\right)^{1/2} e^{i(2kH-\frac{\pi}{4})}\right]F(\theta)\cos\phi \quad (3.31)$$

For the purpose of numerical computation, the principal plane pattern (ϕ=0° plane) is written in the following final form.

$$S^A(\theta) = \frac{F^o(\theta)2i(kd)\sin^2\theta}{\sqrt{2}}e^{-ikA\sin\theta} + \frac{|\cos\theta|\sin(\frac{\phi_o}{2})}{\sqrt{\pi kr_o\sin\theta}}e^{ikr_o}L^o(\theta), \qquad (3.32)$$

$$L^o(\theta) = \frac{e^{i(\frac{\pi}{2}-kA\sin\theta)}}{\sqrt{\pi kr_o\sin\theta}}\left[\frac{2i(kd)\cos^{5/2}\phi_o - 2i\,kd\sin^{5/2}\theta}{\cos\phi_o - \sin\theta} - \frac{e^{ikA\sin\theta}}{\sqrt{1+\sin\theta}}\frac{2i(kd)\cos^{5/2}\phi_o}{\cos\phi_o + \sin\theta}\right], \qquad (3.33)$$

$$S_{12}^P(\theta) = \frac{\pi(kB)^2}{M}\left[2i\,kd\frac{B}{r_1}\frac{e^{ikr_1}}{(kr_1)^2} - 2i\,kd\frac{B}{r_2}\frac{e^{ikr_2}}{(kr_2)^2}\right]F(\theta), \qquad (3.34)$$

$$S_{56}^{P}(\theta) = \frac{i\pi^2 (kB)^2}{2M^2} \frac{e^{ikr_1}}{(kr_1)^2} \frac{(kB)}{(kr_1)}$$

$$\times \left[\left(\frac{1}{\pi kB}\right)^{1/2} e^{i(2kB+\frac{\pi}{4})} - \left(\frac{1}{\pi kH}\right)^{1/2} e^{i(2kH-\frac{\pi}{4})} \right] F(\theta) \quad , \quad (3.35)$$

and the other parameters are as defined before.

3.2 Double Parasitic Loop Counterpoise Antenna Patterns

In the absence of mutual coupling between the parasitic loops, the theoretical expressions for the radiation field produced by a double-parasitic loop system can be obtained by a simple modification of the theory given in Section 3.1.

The far field produced by an antenna consisting of the excited Alford loops, parasitic loop No. 1 and the counterpoise can be written as

$$E_{\phi_1} = \eta_o I_o \left(\frac{ka}{2}\right)^2 \cdot \frac{e^{i(kR-\frac{\pi}{4})}}{R} S_1(\theta) \quad , \quad (3.36)$$

where

$$S_1(\theta) = S^{A}(\theta) + S_{12}^{P}(\theta) + S_{56}^{P}(\theta) \quad (3.37)$$

and all the other notations are as explained in Sect. 3.1. All the parameters involved in the detailed expressions of Eq. (3.31) (see 3.32 through 3.35) should pertain to the parasitic loop No. 1.

Similarly, the far field produced by the parasitic loop No. 2 above the counterpoise can be written as

$$E_{\phi_2} = \eta_o I_o \left(\frac{ka}{2}\right)^2 \frac{e^{i(kR-\frac{\pi}{4})}}{R} S_2^{P}(\theta) \quad , \quad (3.38)$$

where

$$S_2^P(\theta) = S_{12}^{P'}(\theta) + S_{56}^{P'}(\theta) \quad . \tag{3.39}$$

In Eq. (3.39) the terms on the right hand side are given by (3.34) and (3.35) with the understanding that the different parameters involved pertain to the parasitic loop No. 2. Thus the complete far field produced by the non-uniformly excited double parasitic loop counterpoise antenna in the range $0 < \theta < \pi$ is given by

$$E_\phi = \eta_o I_o \left(\frac{ka}{2}\right)^2 \frac{e^{i(kR-\frac{\pi}{4})}}{R} \left[S_1(\theta) + S_2^P(\theta)\right] \quad . \tag{3.40}$$

3.3 Numerical Results

The theoretical expressions given above have been computed numerically to obtain the far field patterns produced by non-uniformly excited single and double parasitic loop counterpoise antennas. One of the typical patterns is shown in Fig. 7. Observe that in Fig. 7 the theoretical field gradient is about 20 dB/6°. Detailed discussions of the numerical and experimental results will be given in a later report.

4. Experimental Investigation

The experimental investigation of the patterns produced by the non-uniformly excited double parasitic loop antenna with 15' diameter counterpoise is in progress. The optimum performance obtained theoretically are being tested experimentally. All these results will be reported later.

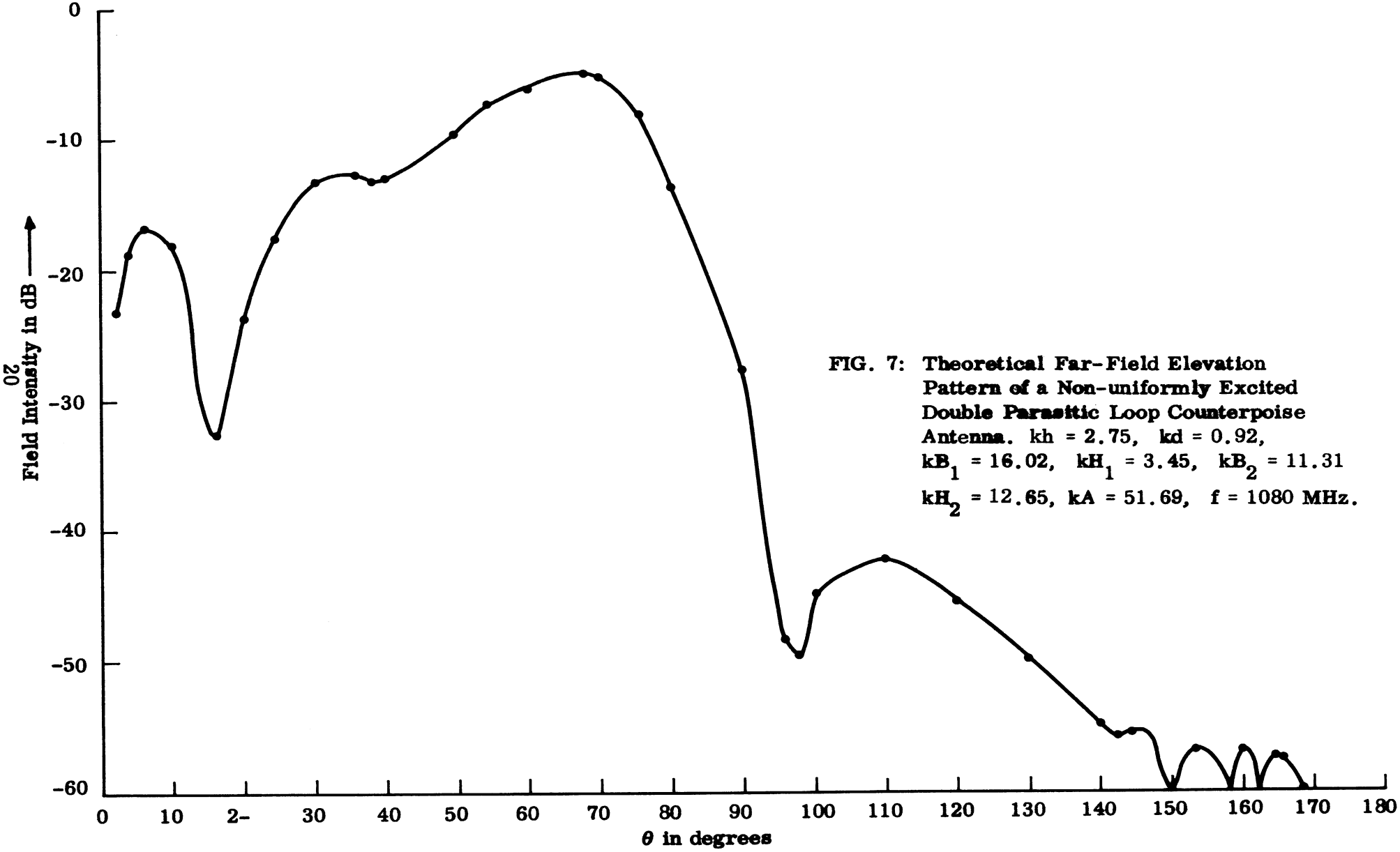

FIG. 7: Theoretical Far-Field Elevation Pattern of a Non-uniformly Excited Double Parasitic Loop Counterpoise Antenna. kh = 2.75, kd = 0.92, kB_1 = 16.02, kH_1 = 3.45, kB_2 = 11.31 kH_2 = 12.65, kA = 51.69, f = 1080 MHz.

5. Conclusions

The above results represent the current status of the theoretical and experimental investigation of the radiation characteristics of non-uniformly excited parasitic loop counterpoise antennas.

The significant contribution during this period has been the development of a satisfactory theory for the existing VOR antennas consisting of Alford loops above a counterpoise. We have also developed a theory for the patterns produced by a non-uniformly excited parasitic loop counterpoise antennas. The theory would be compared with measured results during the coming period.

On the basis of the theoretical results given above and the experimental investigation currently in progress, the design parameters for the full scale double parasitic loop counterpoise antenna will be developed.

6. References

Sengupta, D. L., J. E. Ferris and V. H. Weston (1968), "Theoretical and Experimental Investigation of Parasitic Loop Counterpoise Antennas Final Report," FAA Report SRDS RD-68-50, University of Michigan Radiation Laboratory Report 8905-1-F.

Sengupta, D. L. (1969), "The Radiation Field of a Circular Loop Carrying a Non-Uniform Current," Radiation Laboratory Internal Memorandum 3051-504-M.

Sengupta, D. L., and V. H. Weston (1969), "Investigation of the Parasitic Loop Counterpoise Antenna," IEEE Trans., AP-17, No. 2, pp. 180-191.